Title page:

Improving models of the Earth's magnetic field for directional drilling applications

Authors: Ciarán D. Beggan*, Susan Macmillan, Ellen Clarke and Brian Hamilton

Affiliation: British Geological Survey, Murchison House, West Mains Road, Edinburgh, EH9 3LA, UK

*Corresponding Author: ciar@bgs.ac.uk

Abstract:

Over the past twenty years, directional borehole drilling has become increasingly important for improving the optimal extraction of reserves from challenging targets, for extending the reach of fixed platforms and for reducing wellbore collisions. Very long wells drilled using borehole steering methods can take weeks to months to complete and rely on accurate models of the Earth's magnetic field which necessarily include a parameterization of its time variation. Earth magnetic field models used in the hydrocarbon industry, such as the BGS Global Geomagnetic Model (BGGM), are computed from data collected by a network of ground-based magnetic observatories and from low-Earth orbiting satellites. Magnetic field models provide snapshots looking back in time, but to be useful to industry, they also need to predict how the field will change in the future. Previously, predictions of magnetic field variation have been based on relatively simple extrapolation of the observed changes. We introduce a physics-based technique to forecast the changes in the field by deducing large-scale flow of the iron-rich liquid at the top of the outer core and use this to advect the present magnetic field forwards in time. We demonstrate that this method produces valuable improvements in the accuracy of the BGGM.

Keywords: Potential field Modelling; Magnetics; Downhole

1. Introduction

1.1 Directional drilling

Horizontal directional drilling is the navigation of a wellbore along a pre-designed sub-surface well path to a geological target laterally distant from the rig. It is particularly useful for drilling off-shore and to off-shore locations from on-shore, where targets are typically at a few km depth and greater than 5 km distant horizontally (Figure 1). Extended reach drilling can now achieve well path distances of more than 12 km with the world record of 12.376 km being set by Exxon Neftegas Ltd. in 2012 for well Z-44 in the Chayvo field, Sakhalin, offshore East Russia (Exxon, 2012).

[Figure 1]

The drillers target is contained fully within the geological target and is defined by ellipsoids of uncertainty, derived using sophisticated error models that are now well established within the industry (Williamson, 2000; Miller *et al.*, 2003; ISCWSA, 2009). As demand to maximise hydrocarbon extraction increases, the challenge to the industry to drill safely and cost effectively to small distant geological targets becomes more difficult – particularly within established areas congested with existing wells.

One of the techniques most commonly used is Measurement While Drilling (MWD), where tools are deployed down hole behind the drill bit to measure the gravity and magnetic field vectors. MWD tools typically comprise three orthogonal accelerometers and three orthogonal fluxgate sensors. In MWD, the magnetic field vector is usually described by declination (the angle between magnetic and true north in the horizontal plane), inclination or magnetic dip (the angle between the horizontal and the magnetic field direction) and the total field intensity.

Although significant improvements in tools and survey management processing techniques have taken place (e.g. Lowdon and Chia, 2003; Chia and Lima, 2004), ultimately MWD relies upon measuring the direction of the well-bore relative to the direction of the local geomagnetic field (Russell *et al.*, 1995). Hence accuracy is inherently limited by knowledge of the direction of the Earth's magnetic field at the MWD survey position. This cannot be determined directly from the down-hole data – due to the difficulty in measuring the direction of true north and the noisy magnetic environment – so estimates have to be made using geomagnetic field models.

The desired accuracy requirements on magnetic field values used to correct magnetic MWD data are stringent: 0.1° for declination, 0.05° for inclination and 50 nT for total intensity (at the 95% confidence level) (Russell *et al*, 1995). A study by Macmillan and Grindrod (2010) quantified uncertainties for successive releases of a magnetic field model produced by the British Geological Survey (BGS Global Geomagnetic Model – BGGM). These uncertainties were found to exceed the desired accuracies, hence the need to improve the BGGM.

The magnetic field at any location near the Earth's surface can be expressed as the vector sum of the contributions from three main sources: the main field generated in the Earth's core, the crustal field from the permanently magnetised lithosphere and a combined (external) disturbance field from various electrical currents flowing in the upper atmosphere and magnetosphere.

The main field accounts for approximately 98% of the field strength at the surface of the Earth, and both its spatially varying strength (22,000–67,000 nT) and direction change relatively slowly over time. The crustal and external fields vary in space and time in a manner that is significant enough to warrant inclusion in the magnetic field estimate to meet the accuracy requirements for MWD surveys. These fields are often included in magnetic field estimates for MWD surveys, but in this paper we concentrate on the modelling and forecasting of the main magnetic field.

1.2 Why does the magnetic field change?

The Earth is a compositionally layered body, with a thin crust (5-30 km depth), silicate mantle (30 – 3385 km depth) and iron-nickel core (3385-6371 km depth). The core is approximately the size of Mars and is divided into a liquid outer core and a solid inner core, the latter approximately the size of the Moon (e.g. Lowrie, 2007).

It is generally accepted that the Earth's magnetic field is produced by dynamo action in the outer core. Mechanical energy from flowing liquid iron is converted into electric and magnetic energy (e.g. Lowes, 1984). The driving force that sustains flow and convection in the outer core arises from the buoyancy effects of light element separating out at the outer-inner core boundary. As the fluid material freezes onto the inner core, the lighter elements are squeezed out into the liquid outer core. The relative difference in density means they are buoyant and hence rise to the top of the core. This is believed to account for the majority of the energy available for convection.

The combination of the motion from convection and the relatively rapid rotation of the Earth produces a complex flow regime within the core. However, it is possible to infer the large scale flow from magnetic field measurements if we assume that the magnetic field is entrained into the conductive fluid at the core-mantle boundary over short time scales. The flow therefore helps to create the field but it is also responsible for dragging it along in a process called advection.

The geodynamo is a chaotic system which varies on time scales of months to millennia, including reversing polarity at random intervals. This non-linearity makes it difficult to accurately forecast the change of the magnetic field over a period of more than fifty years and impossible after 1000 years (Hulot *et al.*, 2010). This is analogous to attempting to accurately forecast the weather for periods longer than a week. Therefore to maintain accuracy, the BGGM, for example, is an annually revised geomagnetic field model that contains forecasts of field changes for up to two years following each revision. We discuss this in more detail in the next section.

2 Magnetic Field Modelling

The BGGM is an annually updated model of the Earth's large-scale magnetic field. It consists of (a) a retrospective part up to the present day (e.g. 2013.0), computed from magnetic field data recorded from satellite and ground-based observatories and repeat stations, and (b) a predictive part. It also includes some coefficients describing the large-scale external field.

2.1 Retrospective modelling

The BGGM is a spherical harmonic model derived from predominantly vector geomagnetic field measurements. The magnetic field at any point at or above the Earth's surface can be derived from the following spherical harmonic equation:

$$\Omega(r,\theta,\phi) = \sum_{n=1}^{\infty}\left(\frac{a}{r}\right)^{n+1}\sum_{m=0}^{n}\left(\frac{a}{r}\right)\ \{g_n^m\cos(m\phi) + h_n^m\sin(m\phi)\}P_n^m(\cos\theta) \qquad \text{Equation 1}$$

The magnetic potential (Ω) at any radius (r), latitude (θ) and longitude (ϕ) can be described by a summing series of functions called Legendre polynomials (P_n^m) modified by sine and cosine functions weighted by the so-called Gauss coefficients (g_n^m and h_n^m). *a* is the radius of the Earth. The full field vector (**B**) is calculated from the negative gradient of omega (i.e. $\mathbf{B} = -\nabla\Omega$).

The functions are wavelength-dependent, being modified by the spherical harmonic degree (n) and order (m) summation terms. For example, the main dipole component of the Earth's magnetic field is described using the first three terms: g_1^0, g_1^1 and h_1^1. (Note there is no h_1^0 term, by definition.) Thus, the BGGM consists of sets of Gauss coefficients compactly describing the main field and secular variation.

To create the retrospective part of the BGGM it is necessary to have data with good global coverage, complete coverage in time with as low a noise level as possible. Since the late 1990s the Ørsted and CHAMP satellites (e.g. Olsen and Stolle, 2012) have provided high quality magnetic vector and scalar (i.e. total intensity) data at all latitudes and longitudes, but not during all time periods needed for modelling. This is because the satellites' near-polar orbits precess slowly in local time, i.e. relative to the Sun, and only data collected for a few hours during each night are considered to be relatively free of contamination from difficult-to-model ionospheric signals. Hence, there are periods without any usable satellite data, particularly from Ørsted. These satellite data are augmented with measurements from about 160 ground-based magnetic observatories, which provide complete coverage in time and therefore place constraints on the time variations of the model. Used together, satellite and observatory data provide an exceptional quality dataset for modelling the behaviour of the magnetic field in both space and time.

Prior to the launch of the Ørsted satellite in 1999, only the MAGSAT satellite flying in 1979 and 1980 had provided good quality vector data. Ørsted provided fully calibrated vector data until December 2005, thereafter only total field strength data are available (and now only intermittently). CHAMP, launched in 2000, provided fully calibrated vector data until it de-orbited in September 2010.

In order to further minimise contamination of the model by rapidly varying ionospheric and external field signals, careful selections of both types of satellite data are made. Only data measured during magnetically quiet periods (as determined by magnetic activity indices and solar wind measurements) on the night-side of the Earth are used for modelling. Additional parameters for any remaining large-scale external field are included in the model solution and data which appear to include magnetic fields from sources that are not parameterised are down-weighted appropriately. Satellite data are also weighted according to the measured along-track noise on each orbit.

The contamination of the models by local crustal magnetic fields is minimised by including observatory crustal biases (i.e. the local influence of magnetic rocks) in the model solution. Much of the crustal field signal in the satellite data is attenuated because of the distance of the satellites from the sources (over 600 km altitude for Ørsted and 300 km altitude for CHAMP), but any remaining crustal field that can be robustly modelled is included.

About 3 million data are used to determine many thousands of parameters in the 'parent' magnetic field model. There are many more parameters in the parent model than are necessary for the final BGGM; for example over 5% of the parameters are related to the rapidly varying external field, and many of the small-scale internal field terms are not considered robust. The observatory crustal biases are also not used in the final BGGM.

The parent model is produced from an inversion for the model parameters using an iterative reweighted least-squares process; the iterations being necessary on account of the non-linearity of the data in terms of the model parameters and the assumed uncertainty distribution. More complete descriptions of data selection and model parameterisation for the parent model are in Thomson and Lesur (2007), Thomson *et al.* (2010) and Hamilton *et al.* (2010). Figure 2 (a) shows the final BGGM2013 declination. This is a critical parameter for directional drilling using magnetic MWD. The rate of change of declination also varies across the globe, as shown in Figure 2 (b).

[Figure 2]

2.2 Forecasting methodology

For the predictive part of the model we start by assuming that the magnetic field lines of the main field are essentially 'frozen' into the liquid at the top of the outer core and are therefore advected by the fluid motion. It is then possible to deduce the flow causing the observed field change at the surface of the Earth by examining the relative changes over a period of, say, a year. In reality the magnetic field change is controlled by a balance between processes which cause advection and processes that cause natural diffusion of the field e.g. due to electrical resistance in the mantle.

At large scales, advection dominates diffusion on short timescales (< 10 years) (e.g. Holme, 2007). However, at some sufficiently small length scale, diffusion does become important again – otherwise the geodynamo could not operate. However for our purposes, we can neglect diffusion, thereby arriving at the so-called 'frozen-flux' induction equation, which describes how flowing fluid advects the magnetic field:

$$\dot{B}_r = -B_r \nabla_{\mathrm{H}} \cdot \mathbf{u} - \mathbf{u} \cdot \nabla_{\mathrm{H}}\, B_r \qquad \text{Equation 2}$$

B_r is the radial part of the magnetic field, $\dot{B}_r$ indicates the first derivative with respect to time, **u** is a vector containing the flow components in the north (θ) and east (ϕ) directions along the surface of the core-mantle boundary and ∇_{H} is the horizontal part of the divergence operator (Whaler, 1986).

Equation 2 essentially states that variations of the field are caused by the fluid pushing the magnetic field. We are interested in solving for the velocity vector (**u**). In addition, we are also interested in the acceleration of the magnetic field (i.e. the rate of change of the variation), $\ddot{B}_r$, so that we model the rate of change of the flow velocity $\dot{\mathbf{u}}$. This can be described by the following equation:

$$\ddot{B}_r = -\dot{B}_r \nabla_{\mathrm{H}} \cdot \mathbf{u} - B_r \nabla_{\mathrm{H}} \cdot \dot{\mathbf{u}} - \dot{\mathbf{u}} \cdot \nabla_{\mathrm{H}} B_r - \mathbf{u} \cdot \nabla_{\mathrm{H}} \dot{B}_r \qquad \text{Equation 3}$$

Taken together, the flow velocity and acceleration can describe the observed spatial change of the main field over time. At large horizontal spatial scales (> 1000 km), an average flow velocity of around 20 km/yr is observed while the flow acceleration has a mean of about 2 km/yr^2.

As the secular variation and acceleration of the magnetic field can be measured at the surface, it remains then to solve for the flow velocity and acceleration using the mathematical relationship between fluid flow and magnetic field. However, the solutions to equations (2) and (3) for $\mathbf{u}$ and $\dot{\mathbf{u}}$ are ambiguous because there are at least two unknowns in each equation (i.e. the velocity/acceleration in the north and east directions) and only one known quantity (secular variation or acceleration). To reduce the ambiguity, additional constraints are required. Strategies aimed at reducing the ambiguity of the core flow solutions have been investigated for several decades. Some impose restrictions on the type of flow that is allowed, while others appeal to physical or mathematical constraints.

We apply a constraint that assumes the flow velocity remains constant (steady) over a short period of time. It can be shown that the solution of a steady flow is unique, as long as at least three time steps are used (Waddington *et al.*, 1995). In a similar manner to steady flow, the steady acceleration of the flow can be deduced by combining the acceleration over a number of years. The steady flow captures the gross large-scale aspects of magnetic field change but does not allow for any rapid short-term features. We therefore add a component of acceleration to give a better description of the non-linear change of the magnetic field.

To start, the Gauss coefficients describing the magnetic field from the retrospective field model are used to compute the secular variation and secular acceleration. The flow and acceleration coefficients are related to the magnetic field via a set of equations which involve integrals of triple products of spherical harmonics and their spatial derivatives and the main field coefficients (Whaler, 1986). The solutions require three damping parameters to impose a spatial smoothness on the resulting steady flow velocity and acceleration solutions. These parameters are selected by running the core flow models back in time and tuning them to best fit magnetic field data from observatories.

As an example of the output from our inversion, Figure 3 shows the secular variation for 2010.0 at the Earth's surface and the resulting flow velocity model at the core mantle boundary. The lower panels show the secular acceleration for 2010.0 at the Earth's surface and the flow acceleration model at the core mantle boundary for that period.
The flow velocity model shows strong westward-directed flows in the Atlantic hemisphere while the Pacific hemisphere has relatively weak flow meaning that the magnetic field changes are larger in the Atlantic hemisphere than elsewhere. The flow acceleration model shows strong acceleration in the Indian Ocean. This area in particular has been observed to have a rapidly changing field over the past decade.

[Figure 3]

Once the steady flow and steady acceleration models have been computed, they can be used to predict the change of the field forwards in time. The forecasting process starts at the last epoch of the main field derived from satellite and observatory data. The new secular variation and secular acceleration values of the *field* at this time are computed from the *flow* velocity and acceleration models. However, as Equations (2) and (3) show, there is a dependence of the secular variation and secular acceleration on the main field itself. Hence the process is non-linear and has to be stepped forwards at a suitably fine time resolution (Beggan and Whaler, 2010).

We therefore advect the field forwards using a time step of one month. Each month a new set of matrices relating flow velocity and acceleration to secular variation and secular acceleration are computed based on the previous month's main field and secular variation coefficients. This generates a set of predicted secular variation and secular acceleration coefficients which are added to the main field coefficients for the new prediction of the main field. As the prediction modifies the main field and secular variation coefficients, the prediction is non-linear, reflecting how the magnetic field is advected by the flow in reality.

Figure 4 shows a notional timeline for the generation of a magnetic field model prediction. The secular variation (2008.5-2012.5) and secular acceleration (2009.0-2012.0) are computed from the main field (2008.0-2013.0). Once the steady flow velocity and acceleration are computed, then the main field forecast begins for 2013.0 to 2015.0, by adding together the secular variation of the field derived from the flow velocity model and the secular acceleration derived from the flow acceleration.

[Figure 4]

Note the steady flow velocity is computed up to spherical harmonic degree and order 13 and the flow acceleration model up to degree and order 8. The prediction of the change of the main magnetic field Gauss coefficients after 2013.0 is up to degree and order 13.

3. Forecasting

The obvious question is: how well does the new method forecast the change of the magnetic field, compared to the previous method used for prediction of the field in the BGGM or in other models? In this section we answer this question using two methods: a retrospective study and a comparison with the International Geomagnetic Reference Field (IGRF) model.

3.1 Retrospective study

We conducted a retrospective study to test how well the flow modelling forecast method compares against the previous method of extrapolation used for the BGGM prior to 2013. To do this, steady flow and steady acceleration models were computed from magnetic field data covering the period 2007 – 2011. We used the flow models to predict the magnetic field change over the following two years from 2011 to 2013. We then compared the new method to the previous extrapolation method using an independent dataset of night-time hourly-mean observatory values when the magnetic field was relatively undisturbed for 2011 and 2012.

In order to compare the forecasted magnetic field to the observed magnetic field, we looked at the standard deviation of the differences between the measurements in the three orthogonal components of the magnetic field at 94 observatories across the globe. As with any natural system there are variations about the mean – in this case related to external magnetic field activity. Hence we should not expect the standard deviation of the forecast differences to be smaller than natural variations of the observatory data.

Table 1 shows the average standard deviation for each component of the measured hourly mean data for 94 observatories. As can be seen in the first column, the variation is largest in the X (North) component of the field (12.3 nT) and smallest in the Y (East) component of the field (5.8 nT).

The standard deviation is calculated for the differences between the flow forecast method and each component at each observatory. These are then averaged over all observatories. The values in the X and Y components (12.6 and 5.9 nT, respectively) are very close to the natural variability of measurements suggesting the forecast is quite accurate over the two year period. The extrapolation technique used in previous BGGMs also shows a good fit to the data (e.g. 15.0 and 6.5 nT in X and Y, respectively) but does not follow the variation as well as the flow technique.

[Table 1]

The conclusion to be drawn from Table 1 is that the flow method using velocity and acceleration has been better able to account for the variation of the magnetic field over the previous two years than the extrapolation method previously used in the BGGM.

3.2 Comparison to the International Geomagnetic Reference Field

We compared the forecast from the BGGM flow technique to the forecast from the eleventh version of the International Geomagnetic Reference Field (IGRF) released in December 2009 (Finlay *et al.*, 2010). This is not an entirely fair comparison as the IGRF model is only updated on a quinquennial basis, compared to the annual update of the BGGM, so we note the differences are more illustrative of the variation of the magnetic field and our current ability to predict it than a critique of the IGRF-11. However we include this comparison here as the IGRF is sometimes used in directional drilling despite its quinquennial update and exclusion of the long-wavelength crustal field.

We used the same process as in Section 3.1 to produce the BGGM prediction of the main field variation. Figure 5 shows the predicted values of the magnetic field at seven globally distributed observatories near hydrocarbon areas. The dots are the hourly-mean measurements made at 02:00-03:00 local time at each observatory. The blue line shows the forecast IGRF values for each component and the red line shows the BGGM flow model forecast. Note that the red and blue lines have had the mean crustal bias in each component at each observatory removed in order to show how the difference from the observatory data varies with time. Figure 5 shows that the forecast from both models is reasonably good but, overall, the BGGM achieves better results due to having additional data up to 2011.0 and through using the flow forecast method.

Finally, to make the point about updating the model annually, in Figure 6 we present the global differences between the IGRF-11 forecast made in 2009.5 for 2011.0 to 2015.0 and that of BGGM2013 but truncated to the same maximum spherical harmonic degree of the IGRF (13). Note, BGGM2013 includes magnetic field data up to 2013.0 and makes a forecast to 2015.0. As can be seen the differences become much larger over time, mainly due to the acceleration of the field around the southern Atlantic and North America. The IGRF model has not captured these changes.

[Figure 5]

[Figure 6]

4. Conclusion

Improvements in the modelling of the geomagnetic field complements other MWD improvements developed over the past few decades, providing more accurate well bore surveys and better estimation of positional uncertainty.

The implementation of core flow modelling into the forecasting methodology of the BGGM has been shown to bring a worthwhile improvement. Core flow modelling can be considered a smoothing technique and hence can be seen as capturing the average changes of the motions of the fluid outer core. However, the method requires damping parameters which are dependent on the era and thus, expert input is required to maintain this modelling improvement year by year.

A retrospective analysis of the period 2011.0-2013.0 shows that the steady flow and acceleration modelling generates relatively good forecasts of the field change. Therefore, this suggests that the use of a steady flow and acceleration model for forecasting the change of the magnetic field over short periods of time for future releases of the BGGM is worthwhile and this method has now been implemented for the 2013 release of the BGGM. In order to maintain confidence in the accuracy, each year the forecast from previous revisions will be checked against available observatory data and tuned to provide the best retrospective fit.

Further improvements in field accuracy will allow a reduction in the size of the error ellipsoid providing a larger driller’s target for any given geological target. This should increase confidence and reduce drilling time – producing cost savings whilst maximising the potential for hydrocarbon production.

References:

Beggan, C., and Whaler, K. [2010] Forecasting secular variation using core flows. *Earth Planets and Space*, 62, 821-828.

Chia, C.R. and de Lima, B.C. [2004] MWD Survey Accuracy Improvements Using Multistation Analysis, *Society of Petroleum Engineers*, Paper 87977

Exxon Neftegas Limited, Sakhalin-1 Project Breaks Own Record for Drilling World`s Longest Extended-Reach Well, http://www.sakhalin1.com/Sakhalin/Russia-English/Upstream/media_news_events_Z44.aspx [accessed 01-July-2013]

Finlay, C. C., Maus, S., Beggan, C. D., Bondar, T. N., Chambodut, A., Chernova, T. A., Chulliat, A., Golovkov, V. P., Hamilton, B., Hamoudi, M., Holme, R., Hulot, G., Kuang, W., Langlais, B., Lesur, V., Lowes, F. J., Lühr, H., Macmillan, S., Mandea, M., McLean, S., Manoj, C., Menvielle, M., Michaelis, I., Olsen, N., Rauberg, J., Rother, M., Sabaka, T. J., Tangborn, A., Tøffner-Clausen, L., Thébault, E., Thomson, A. W. P., Wardinski, I., Wei, Z. and Zvereva, T. I. [2010] International Geomagnetic Reference Field: the eleventh generation. *Geophysical Journal International*, 183, 1216–1230. doi: 10.1111/j.1365-246X.2010.04804.x

Hamilton, B., Macmillan, S. and Thomson A.W.P. [2010] The BGS magnetic field candidate models for the 11th generation IGRF. *Earth Planets and Space*, 62, 737-743.

Holme, R. [2007] Large-scale flow in the core. *Treatise on Geophysics,* 8, 107-130.

Hulot, G., Lhuillier, F. and Aubert, J. [2010] Earth's dynamo limit of predictability. *Geophysical Research Letters*, 37, L06305, doi:10.1029/2009GL041869.

Industry Steering Committee on Wellbore Survey Accuracy (ISCWSA) [2009]MWD Error Model Revision 3, http://copsegrove.com/MWDModel.aspx [accessed 01-July-2013]

Lowdon, R.M. and Chia, C.R. [2003] Multistation Analysis and Geomagnetic Referencing Significantly Improve Magnetic Survey Results, *Society of Petroleum Engineers*, Paper 79820.

Lowes, F. J. [1984] The geomagnetic dynamo-elementary energetics and thermodynamics. *Geophysical Surveys*, 7, 91-105.

Lowrie, W. [2007] *Fundamentals of Geophysics,* Cambridge University Press, 2nd edition.

Macmillan, S. and Grindrod, S. [2010] Confidence limits associated with values of the Earth's magnetic field used for directional drilling. *SPE Drilling & Completion*, 25(2), 230-238. doi: 10.2118/119851-PA.

Miller, R., Terpening, M. and Conran, G. [2003] Survey Management Provides A Safer Drilling Environment With Reduced Drilling Costs, *American Association of Drilling Engineers National Technology Conference*, AADE-03-NTCE-19

Olsen, N. and Stolle, C. [2012] Satellite Geomagnetism, *Annual Review of Earth and Planetary Sciences*, 40, 441-465, doi: 10.1146/annurev-earth-042711-105540

Russell J.P., Shiells G., and Kerridge D.J. [1995] Reduction of Well-bore Positional Uncertainty Through Application of a New Geomagnetic In-Field Referencing Technique, *Society of Petroleum Engineers*, Paper 30452.

Thomson, A. W. P., Hamilton, B., Macmillan S. and Reay, S. J. [2010] A novel weighting method for satellite magnetic data and a new global magnetic field model. *Geophysical Journal International*, 181, 250-260, doi: 10.1111/j.1365-246X.2010.04510.x.

Thomson, A. W. P. and Lesur, V. [2007] An improved geomagnetic data selection algorithm for global geomagnetic field modelling. *Geophysical Journal International*, 169, 951–963 doi: 10.1111/j.1365-246X.2007.03354.x.

Waddington, R., Gubbins, D. and Barber, N. [1995] Geomagnetic field analysis V: Determining steady core flows directly from geomagnetic observations. *Geophysical Journal International,* 122, 326–350.

Whaler, K. A. [1986] Geomagnetic evidence for fluid upwelling at the core-mantle boundary. *Geophysical Journal of the Royal Astronomical Society*, 86, 563-588.

Williamson, H S. [2000] Accuracy Prediction for Directional Measurement While Drilling, *Society of Petroleum Engineers*, Paper 67616.

List of Captions

Figure 1: Horizontal drilling in a complex environment

Figure 2: Global map of (a) declination angle and (b) the rate of change of declination angle

Figure 3: Core flow velocity derived from secular variation of the magnetic field radial component for 2010.0 (upper panel); core flow acceleration derived from secular acceleration of the radial component for 2010.0 (lower panel). Continents are shown for reference only on the flow plots.

Figure 4: Timeline for magnetic field forecasting. The flow velocity and acceleration models are derived from the secular variation and acceleration of the main field prior to the forecast period. They are used to compute the changes to the main field over the following two years after 2013.

Figure 5: Comparison of the prediction of a retrospective BGGM model with core flow (red line) with the prediction from the IGRF-11 model (blue line) against actual measurements from ground-based observatories (black dots). Jim Carrigan (JCO), Alaska; Lerwick (LER), UK; Sable Island (SBL), offshore Nova Scotia, Canada; Phuthuy (PHU), Vietnam; Learmouth (LRM), Northwest Australia; Canberra (CNB), Australia; Port Stanley (PST), Falkland Islands.

Figure 6: Global differences between BGGM2013 and IGRF-11 for 2011.0 and 2013.0 and the predicted differences for 2015.0 in the X (North), Y (East) and Z (vertical) components of the magnetic field.

Table 1: Average standard deviation of 94 observatory hourly-mean values and the average standard deviation of the difference between the observatory values and the forecasts from the flow method and the extrapolation method.

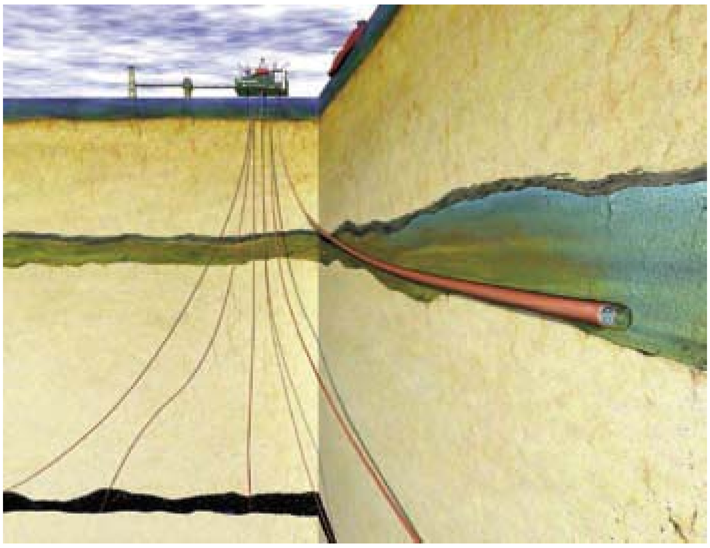

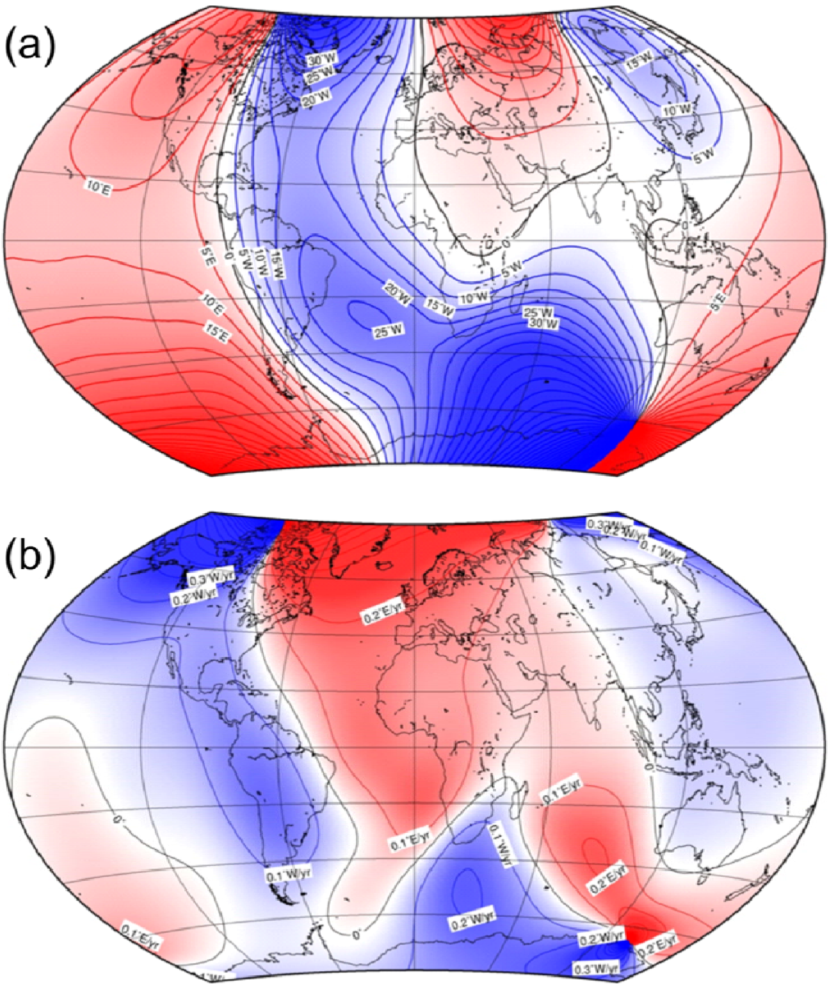
(a)
30°W
25°W
20°W
15°W
10°W
5°W
10°E
5°E
15°E
0°
25°W
30°W
(b)
0.3°W/yr
0.2°W/yr
0.2°E/yr
0.1°W/yr
0.1°E/yr
0.2°E/yr
0.2°W/yr
0.3°W/yr
0°

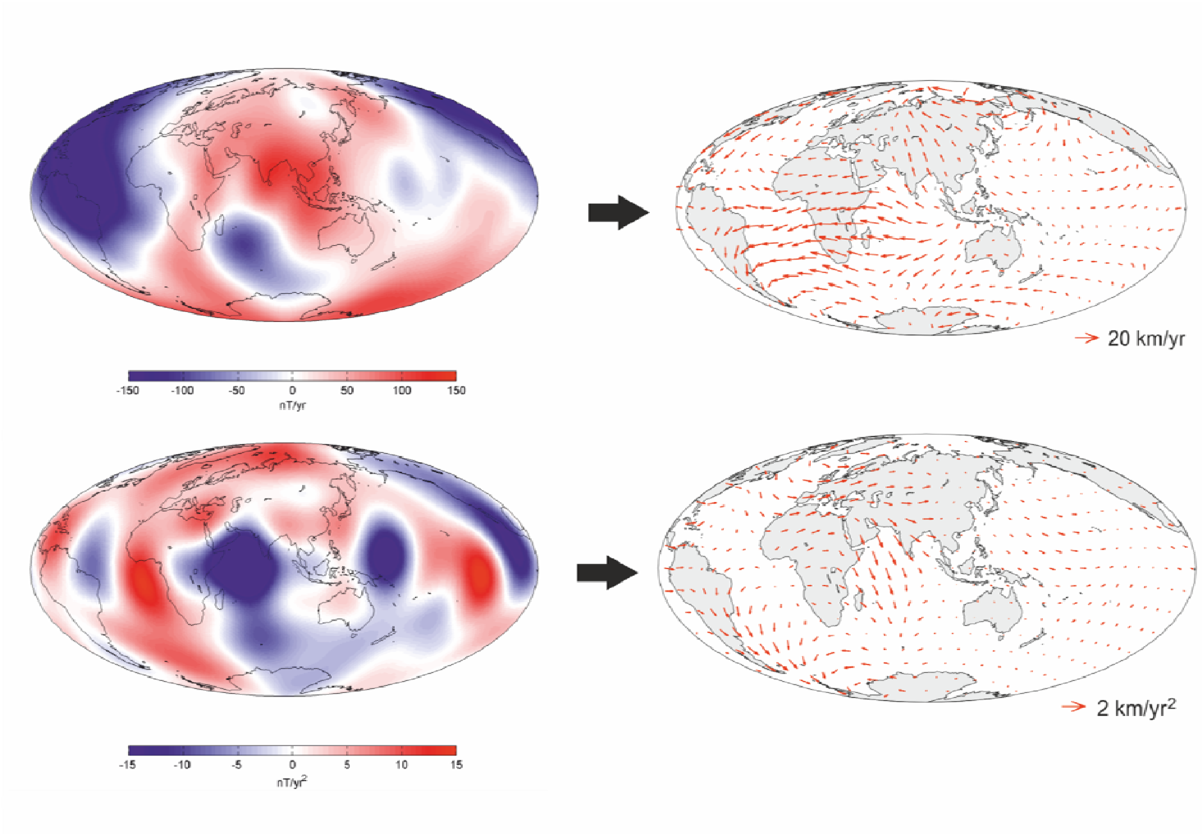
20 km/yr
-150 -100 -50 0 50 100 150
nT/yr
2 km/yr^2
-15 -10 -5 0 5 10 15
nT/yr^2

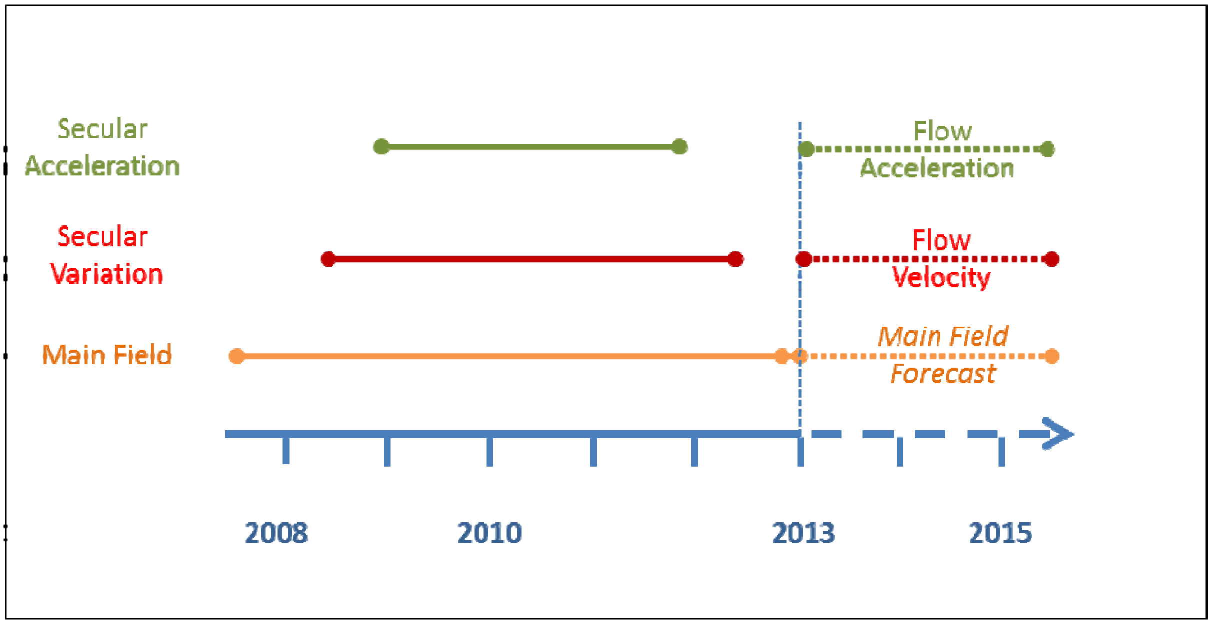
Secular Acceleration
Flow Acceleration
Secular Variation
Flow Velocity
Main Field
Main Field Forecast
2008
2010
2013
2015

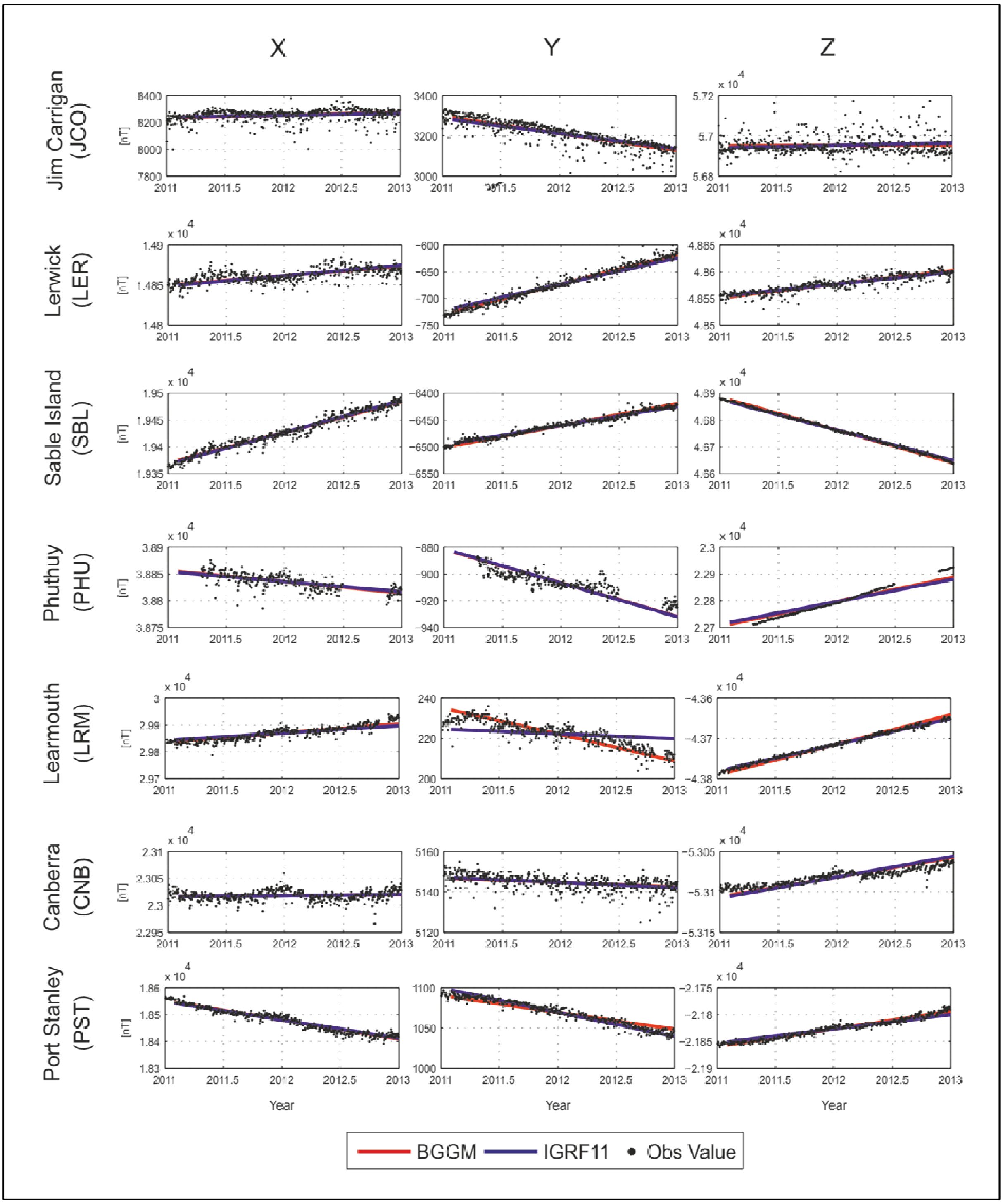
X
Y
Z
Jim Carrigan (JCO)
Lerwick (LER)
Sable Island (SBL)
Phuthuy (PHU)
Learmouth (LRM)
Canberra (CNB)
Port Stanley (PST)
[nT]
Year
BGGM
IGRF11
Obs Value

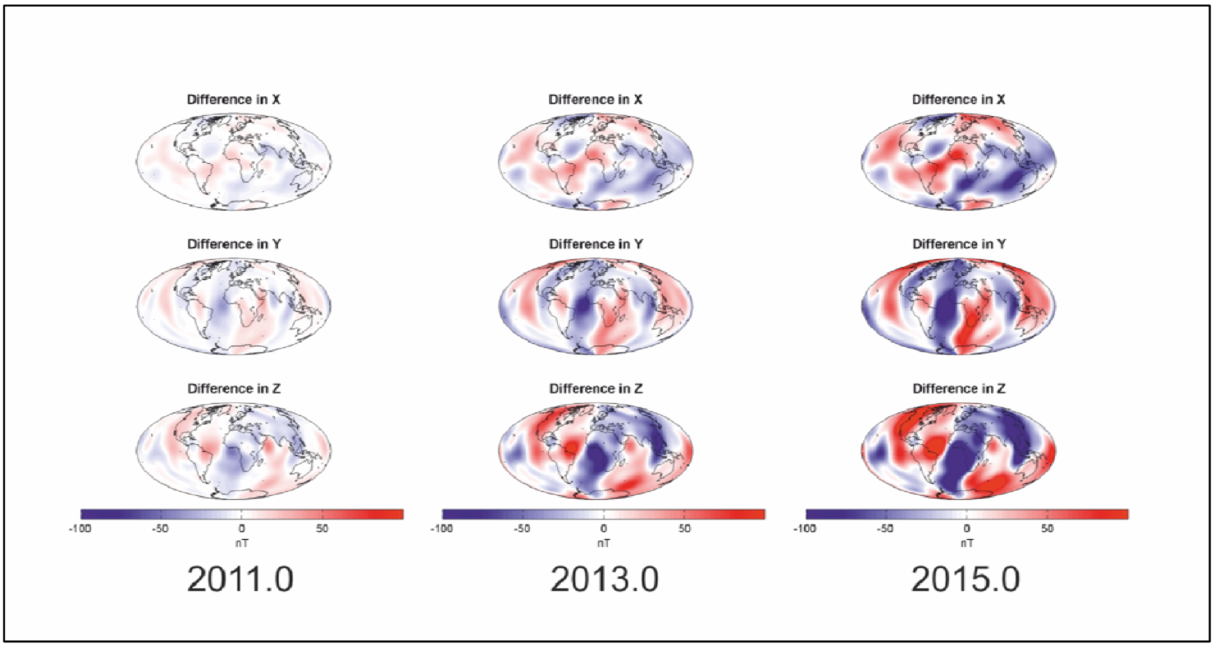
Difference in X
Difference in X
Difference in X
Difference in Y
Difference in Y
Difference in Y
Difference in Z
Difference in Z
Difference in Z
-100 -50 0 50
nT
-100 -50 0 50
nT
-100 -50 0 50
nT
2011.0
2013.0
2015.0

Component	Average of standard deviation (nT)		
	Observatory	**Flow method**	**Extrapolation method**
X	12.3	12.6	15.0
Y	5.8	5.9	6.5
Z	7.3	8.2	10.8